Applied Surface Science 656 (2024) 159694

Contents lists available at ScienceDirect

Applied Surface Science

journal homepage: www.elsevier.com/locate/apsusc

Full Length Article

Investigation of the influence of aluminum surficial water on aluminum-plastic hybrids through a combined experimental and simulation approach

Shuaijie Zhao [a], Chuantong Chen [a,*], Hang Liang [b,*], Shuohan Wang [c], Fuminobu Kimura [c], Yusuke Kajihara [c]

[a] SANKEN, Osaka University, Osaka, Japan
[b] School of Material Science and Engineering, Tianjin University, Tianjin 300072, China
[c] Institute of Industrial Science, The University of Tokyo, 4-6-1 Komaba, Meguro-ku, Tokyo 153-8505, Japan

ARTICLE INFO

Keywords:
Metal-plastic hybrid
Surficial adsorbed water
Molecular dynamics
Hybrid bonding

ABSTRACT

Aluminum-plastic hybrid joints have become increasingly important due to weight reduction in the engineering field. Previous studies claimed that aluminum surface conditions are critical for the hybrids. However, the influence of the surficial adsorbed water, which always covers the aluminum surface at normal ambient conditions, is rarely known. This paper investigated the influence of the surficial adsorbed water through a combined experimental and simulation approach. We prepared aluminum plates with different surficial adsorbed water amounts and fabricated aluminum/polyamide 6 (PA6) hybrids. The bonding strength was measured. The aluminum surface was characterized by various methods to understand its surficial adsorbed water conditions. Molecular dynamics were also performed and compared with experimental results. The results clarified that the surficial adsorbed water influences the bonding strength of metal-plastic hybrids greatly at a molecular level, which will significantly contribute to the knowledge of metal-plastic hybrids.

1. Introduction

Recently, the metal-plastic direct bonding technique has become gradually important because of the increasing need for weight reduction in many engineering fields. Besides weight reduction, metal-plastic direct bonding methods improve production efficiency greatly and offer a more flexible design by eliminating screws and adhesives used in conventional methods [1,2].

The successful bonding of the metal and plastic is believed to contribute from the mechanical anchoring effect [1], Van der Wall's force [3,4], electrostatic force [3,4], hydrogen bond [5], or chemical bond [6,7] between metal and plastic. The mechanical anchoring effect is produced by the infiltration of plastic into metal surface structures. The Van der Wall's force generally exists between metal and plastic as long as there is no gap between metal and plastic at the interface. The electrostatic force is the attractive or repulsive force between particles that are caused by their electric charges. The hydrogen bond can be produced between the polar groups on a metal surface and the functional groups in the plastic. Chemical bonding is also possible between metal and plastic by reaction between metal ions and free radicals in the plastic. The chemical bond is the strongest bond, followed by the hydrogen bond, but the chemical bond is much more difficult to form.

A key evaluation metric for the metal-plastic hybrids is the bonding strength. In previous studies, many researchers improved the bonding strength by optimizing the mechanical anchoring effect, like making deeper surface structures [1], making a combination of micro and nano structures [8], etc. Recently, several studies reported that the formation of chemical bond/hydrogen bonds between metal and polymer improved the bonding strength significantly [5–7]. Since the bond strength of the chemical bond/hydrogen bond is several times the Van der Wall's force and the electrostatic force, the formation of chemical bond/hydrogen bond at the metal/plastic interface would be a potential way to improve the bonding strength.

However, the formation of chemical bond/hydrogen bond is not an easy task. Except for the reactivity between metal and plastic, close contact between metal and plastic is required because the premise of the chemical bond/hydrogen bond is the close distance, usually less than 0.35 nm. High pressure is usually applied during metal-plastic direct

* Corresponding authors.
E-mail addresses: chenchuantong@sanken.osaka-u.ac.jp (C. Chen), hangliang@tju.edu.cn (H. Liang).

https://doi.org/10.1016/j.apsusc.2024.159694
Received 30 October 2023; Received in revised form 16 January 2024; Accepted 10 February 2024
Available online 13 February 2024

bonding to obtain close contact. However, high pressure only seems not enough. This is because many previous studies [9–12] show that the metal surface is easy to have physiosorbed/chemisorbed water or organic contamination, blocking the close contact between metal and plastic. Al-Abadleh [9] and Rubasinghege [10] showed that water adsorbs on the metal surface in an ordered fashion with the formation of a stable hydroxide layer. It indicates that water adsorption is also possible to change surface chemical conditions by hydroxylation of metal surficial oxides, making the water adsorption more stable. Van den Brand [11] found that the absorption of water reduced the capacity of oxide surfaces to bond with myristic acid. Yoshizawa [12] also showed that surficial water reduced the adhesion between aluminum and epoxy by using molecular dynamics (MD). The detrimental effects of surficial water on bonding were also investigated by Cui [13] and Sun [14]. These studies implied that the surficial adsorbed water may influence the bonding strength of metal-plastic hybrids greatly. However, the influence of the surficial adsorbed water on the metal-plastic hybrids was rarely investigated.

Therefore, this study aims to understand the influence of aluminum surficial adsorbed water on the bonding strength of metal-plastic hybrids. We used a combined experimental and simulation approach. We used aluminum as the metal part and polyamide 6 (PA6) as the plastic part. Aluminum plates with different amounts of surficial adsorbed water were prepared by heating aluminum plates at high temperatures for different times. We analyzed the water amount by various methods. The aluminum/PA6 hybrids were made by injection insert molding. Then, we measured the bonding strength changes to evaluate the influence of the surficial adsorbed water. AFM-IR was used to characterize the bonding interface. MD simulations were performed in parallel. The experimental and simulation results were compared and discussed. Our work is expected to provide a fresh insight into the aluminum surficial adsorbed water's influence on the metal-plastic hybrids.

2. Experimental

2.1. Materials

We used annealed A5052 aluminum alloy plates as metal parts (length:45 mm, width:18 mm, thickness:1.5 mm) and injected molded PA6 plates as plastic parts (length:50 mm, width:10 mm, thickness:3 mm). The material properties of A5052 and PA6 are listed in Table 1.

2.2. Surface treatment and injection molding

Producing aluminum surfaces containing different amounts of surficial adsorbed water is critical for this study. A previous study [11] used an accumulated way by placing the aluminum surface in a humid environment for different times to increase the surficial water. In this study, we used a reducing way that is heating the aluminum surface in high temperatures to reduce the amount of surficial adsorbed water because the reducing way takes less time and produces minor influence on surface structures.

Additionally, one important point is that we need to exclude the influence of hydroxylation by water [10]. It is widely known that aluminum oxide (Al_2O_3) covers the aluminum surface. This Al_2O_3 surface is easy to become hydroxylated in the presence of water, and this hydroxylation is influential for surface structures/chemical conditions and subsequent hybrid bonding [15]. If hydroxylation happens, it is difficult for us to distinguish whether the influence results from the surficial water or the hydroxylation caused by water. To achieve this objective, we first fully hydroxylated the A5052 plates by boehmite treatment [16]. The boehmite treatment is a treatment that immerses the aluminum plate in high-temperature water to hydroxylate the aluminum surface by producing amorphous boehmite (AlOOH) structures on the aluminum surface. We performed boehmite treatment in the following procedures. We first removed the original contaminated oxide on A5052 plate by alkaline etching and acid etching, followed by washing the plates in DI water. Then, the A5052 plate was immersed in deionized water at 95 °C for 5 min to form boehmite (AlOOH) on the aluminum surface [16,17]. Since the boehmite treatment was performed in water, surficial adsorbed water should cover the nanostructures on the aluminum surface. We will characterize this in later sections. To produce A5052 surface having different amounts of surficial adsorbed water, we heated boehmite-treated A5052 plates at 250 °C for 10 min and at 500 °C for 10 min. We selected such high temperatures because several previous studies [18,19] showed that total desorption of water from metal oxide surfaces required a heating temperature over approximately 450 °C. In this way, we prepared the aluminum surfaces with different surficial adsorbed water. In addition, previous studies [20] showed that boehmite had obvious structures change and decomposition at 600 °C. The boehmite structure became unstable at temperatures over 425 °C for two hours. Therefore, a short heating time is necessary to avoid structure change of boehmite. This is why we selected 10 min. The change in boehmite structures and chemical conditions will be shown in later sections.

Then, we joined the treated A5052 plates with PA6 by using injection insert molding. Before injection molding, PA6 pallets were baked at 120 °C for 5 h to remove the adsorbed water. The joined sample is schematically shown in Fig. 1. Aluminum plate was set in the mold. After mold closure, melted PA6 was injected into the cavity at a flow speed of 10 mm/s with a momentary maximum pressure of 100 MPa to make the melted PA6 close contact with the aluminum surface. Then, a holding pressure of 50 MPa was applied to compensate for the plastic shrinkage. During the molding process, the mold temperature was set to 140 °C. After that, the molded hybrid was ejected from the mold for bonding strength measurement.

2.3. Characterization

The amount of surficial adsorbed water was characterized with X-ray photoelectron spectroscopy (XPS, PHI 5000 VersaProbe, ULVAC-PHI). We performed the precise scan for O1s with a monochromatic Al Kα X-ray source (1486.6 eV) at 25 W. The orientations of the analyzer axis and source axis were set to 90° and 45° to the sample surface. The obtained spectrums were analyzed with CasaXPS. The C1s peaks of all

Table 1
Material properties.

Properties of A5052	
young's modules	69.3 GPa
yield strength	90 MPa
tensile strength	195 MPa
linear expansion coefficient	2.4 × 10^{-5}/°C
Properties of PA6 CM1011G-30	
reinforced	Glass fiber 30 %
tensile strength	185 MPa
linear expansion coefficient	2–3 × 10^{-5}/°C
melting point	225 °C

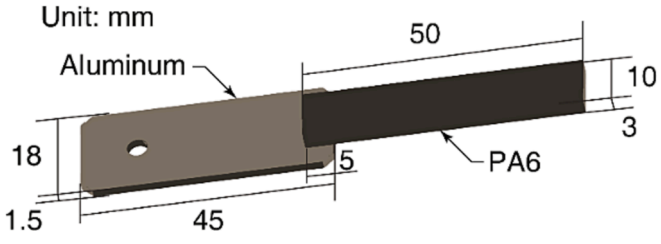

Fig. 1. Geometry of a metal–plastic hybrid.

spectrums were calibrated by shifting to 284.8 eV to avoid the charging effect. A Shirley-type background was used to fit the peaks.

We also analyzed the surface with Time-of-Flight Secondary Ion Mass Spectrometry (ToF-SIMS, M6, IONTOF). We measured the depth information of the treated A5052 plates with the ToF-SIMS running at a chamber pressure of 1.0×10^{-7} Pa. The depth information was measured by performing secondary ion analysis and sputtering over and over for 10 s. Positive ions were measured for the secondary ion analysis. They are produced by a 25 keV Bi^{+++} liquid metal ion gun with a 1.2 pA current over a 100×100 μm^2 area. Sputtering was done by a 20 keV Ar^+ gas cluster ion beam with a 17nA target current over a 400×400 μm^2 area. Both liquid metal ion gun and gas cluster ion beam have an incident angle of 45°.

The surface structures of the treated A5052 plates were observed with a Scanning Electron Microscope (SEM, S-4800, Hitachi High Technologies) and an Atomic Force Microscope (AFM, L-trace II, Hitachi High Technologies) to observe whether heating causes structures change of boehmite or not. We took SEM images with a 10 k magnification under an accelerating voltage of 5 kV. For AFM measurement, dynamic force mode and a cantilever with a tip diameter of 10 nm were used. An area of 500 nm × 500 nm (256 px × 256 px) was scanned for each sample.

The tensile shear strength of the aluminum/PA6 hybrid was measured via a universal tensile testing machine (AGS-X, Shimadzu) at a tensile speed of 1 mm/min. Five samples were measured to obtain the average bonding strength.

Moreover, the surficial adsorbed water's influence on the hydrogen bond/chemical bond is of great importance because this influences the bonding strength significantly. However, since this bond only exists at the aluminum/PA6 interface in a nanoscale, it is difficult to be detected. Here, we applied a new chemical characterization method, Atomic Force Microscopy-based Infrared Spectroscopy (AFM-IR, nanoIR2, Bruker), to characterize the influence of surficial adsorbed water on the hydrogen bond/chemical bond between aluminum and PA6. Unlike the general IR system, AFM-IR enables the nano-scale IR spectrum measurement. The probe of AFM, which has a tip diameter of 10 nm, locates the position needed to measure. Then, a pulse laser radiates the position under the AFM probe. If the frequency of the incident radiation meets a specific molecular resonance in the sample, the sample absorbs the laser radiation and becomes heated. The heat causes a rapid thermal expansion pulse of the sample and then excites the resonant oscillation of the AFM cantilever. The oscillation is then transformed into IR spectrums. The detailed principle of the AFM-IR can be found in our previous study [5]. Theoretically, AFM-IR is capable of measuring the spectrum in a 10 nm area. In this study, the spectrums under the range of 1000–2000 cm^{-1} were taken at a resolution of 4 cm^{-1}.

3. Simulations

This paper used Winmostar [21] to build atomic models and used Large-scale Atomic/Molecular Massively Parallel Simulator (LAMMPS) [22] to perform molecular dynamics simulations. Since there is no specific force filed to describe the interaction between AlOOH, surficial adsorbed water, and PA6 currently, we used general force fields. Buckingham potential is used for AlOOH; General AMBER Force Field (GAFF) is used for PA6; the extended simple point charge (SPC/E) water model is used for surficial adsorbed water. The interaction between AlOOH, PA6, and surficial adsorbed water is described by Lennard-Jones potential and Coulomb potential. For all the simulations in this study, Van der Walls interactions based on atom summation with a cutoff of 15 Å, electrostatic interaction based on Ewald summation method with a cutoff of 15 Å, and a time step of 0.5 fs were used.

Fig. 2(a) shows the models for the amorphous AlOOH, surficial adsorbed water, and PA6. The detailed modeling processes for each model are described as follows.

The amorphous AlOOH model was built by the method proposed by Adiga [23]. 1000 aluminum atoms with a charge of 1.4175, 2000 oxygen atoms with a charge of −0.945, and 1000 hydrogen atoms with a charge of 0.4725 were put into a simulation box with a dimension of 50 Å × 50 Å × 18 Å. We first heated this system to 1000 K and equilibrated it for 50 ps under NVT ensemble. This was followed by quenching the systems to 300 K in a total time of 50 ps. Then, we built a 50 Å vacuum space along the Z axis to build the surface. After that, the surface model was again heated to 1000 K and quenched to 300 K for 50 ps, respectively.

The surficial adsorbed water model was set to have the same length as the amorphous AlOOH model in X and Y directions. The water molecule numbers were adjusted to simulate the influence of water amount. We simulated 0, 200, 400, 600 water molecules. The corresponding length in Z-axis for the water model was 0, 3, 6, and 9 Å, respectively.

The PA6 model was set to have the same length as the amorphous AlOOH model in X and Y directions. The PA6 model contains 40 chains. Each chain consists of 20 PA6 monomers. The PA6 model was first equilibrated at 1000 K and 1 atm under NPT ensemble for 50 ps and then equilibrated at 300 K and 1 atm under NPT ensemble for another 50 ps.

After building these three models, we stack them together, as shown in Fig. 2(b), to simulate the surficial adsorbed water and the bonding

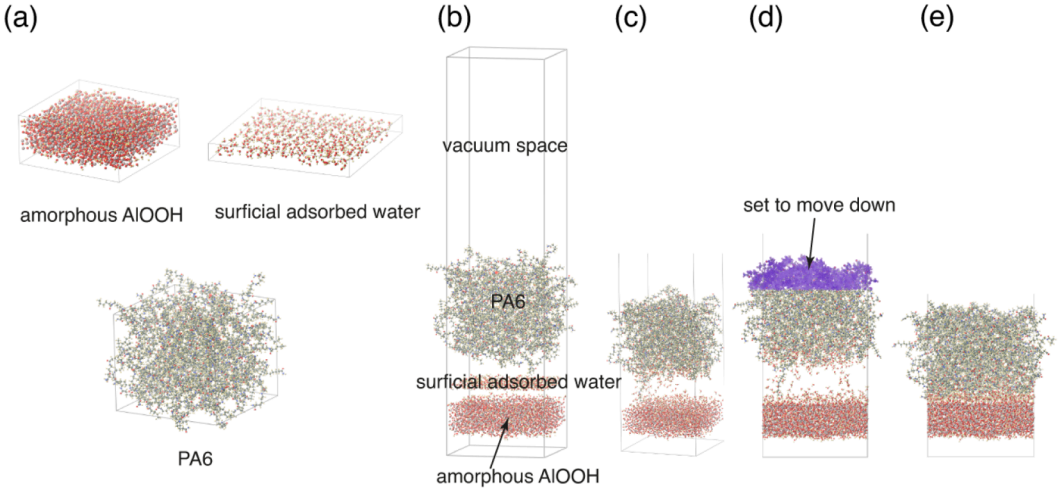

Fig. 2. (a) the models for the amorphous AlOOH, surficial adsorbed water, and the PA6; (b) the stacked model; (c) the results after equilibration of the stacked model at 500 K; (d) the results after simulating the packing; (e) the results after equilibration again at 500 K and 300 K.

interface. A vacuum space above the PA6 model is built by extending the simulation box length in Z axis to 200 Å to eliminate the cross-periodical boundary effect. To save computation time, we fixed the amorphous AlOOH model. The system was first equilibrated at 500 K for 50 ps. The equilibrated results are shown in Fig. 2(c). We selected this temperature because the sensor in the mold showed a temperature of 500 K during the injection molding. To simulate the compression by the packing pressure during injection molding, part of the molecules in the PA6 model, as shown in Fig. 2 (d), was set to move down at a speed of −0.002 Å/fs for 25 ps. After the compression, the system was equilibrated at 300 K for 100 ps. The final equilibrated result is shown in Fig. 2 (e).

Adhesion energy was used to evaluate the surficial adsorbed water's influence on the bonding between aluminum and PA6. The calculation of adhesion was based on an equation below, which is proposed by [13,14]. The larger the adhesion energy, the better the bonding between aluminum and PA6.

$$E_{adhesion} = -E_{interaction-\frac{Al}{PA6}} = -(E_{total} - (E_{Al} + E_{PA6}))$$

The distribution of water molecules and the formation of hydrogen bonds between the amorphous AlOOH and the PA6 were also discussed.

4. Results and discussion

4.1. Surface analysis

We first need to confirm whether the proposed surface treatment method successfully produced the surfaces with different amounts of surficial adsorbed water. Here, we confirmed this with XPS and ToF-SIMS.

Fig. 3 shows XPS precise scan results for O1s. The peak fitting for O1s was based on the methodology proposed by McCafferty [24]. Three O1s peaks belonging to surficial adsorbed water, –OH, and oxide ion (O^{2-}), were detected, which well fits McCafferty's results. It shows that the surficial adsorbed water existed for all three surfaces, but its percentage was reduced by the heating, as listed in Table 2. With higher heating temperatures, more reduction of surficial adsorbed water was observed. Previous studies [18,19] indicated that such high temperatures should reduce the surficial adsorbed water amount by 80–90 %, but the results here show that the amount only reduced by 50 %. This difference should be caused by the water absorption in the atmosphere after heating. Although we protected the aluminum plates in a nitrogen-filled case after heating and performed XPS measurements as soon as possible, it was unavoidable for the aluminum plates to come into contact with the atmosphere during the XPS sample preparation. It is supposed that atmospheric water was adsorbed by the aluminum plates again. Nevertheless, XPS results show that we obtained aluminum surfaces with different amounts of surficial adsorbed water, which is sufficient for our investigation. Also, such surfaces are more suitable for simulating the practical molding process because the aluminum plates are exposed to the atmosphere during the injection molding process before mold closure. Table 2 also shows that the ratio of –OH to O^{2-} was near 1, indicating that these surfaces were composed of AlOOH. Also, it shows that after heating at 500 °C, the ratio of –OH to O^{2-} was also near 1.

Table 2
Atomic percentage of surficial water, –OH, O^{2-} on the surfaces.

Condition	at. % H_2O	at. % OH	at. % O^{2-}	Ratio of –OH to O^{2-}
without heating	6.80	28.62	30.25	0.95
heating at 250 °C	5.85	29.99	31.08	0.96
heating at 500 °C	3.65	26.44	28.37	0.93

XPS evaluates the amount change, while ToF-SIMS provides both amount and thickness information, which helps us to better understand the surficial adsorbed water. Fig. 4 shows the depth profile of the H_3O^+ for the different surfaces. The existence of the fragment of H_3O^+ indicates the existence of surficial adsorbed water. The area below the intensity curve can be regarded as an indicator of the total amount of surficial adsorbed water. Like XPS, ToF-SIMS also shows that the amount reduced with the increased heating temperature. Also, ToF-SIMS depth profile shows that the thickness of the surficial adsorbed water reduced after heating at 250 °C and reduced more after heating at 500 °C. The results suggest that surficial adsorbed water exists in multiple layers. Also, the results show that heating not only reduces the water amount but also reduces the thickness of the surficial adsorbed water.

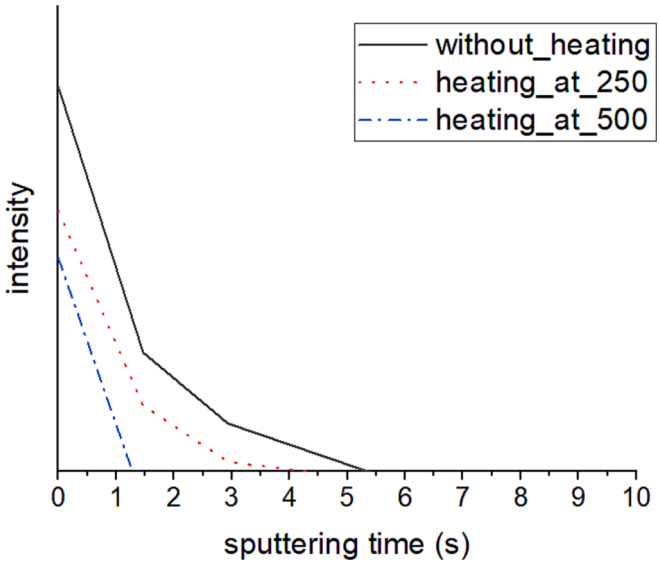

Fig. 4. ToF-SIMS intensity results of H_3O^+ for the surfaces with different water amounts.

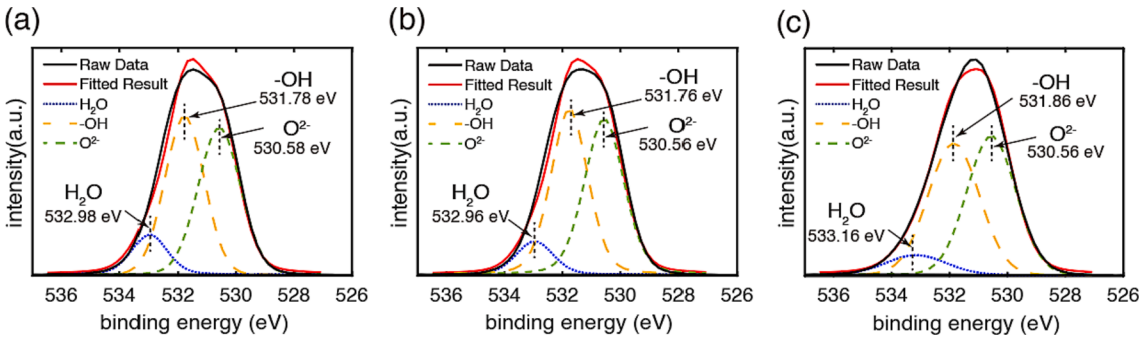

Fig. 3. Fitted O1s narrow scan results for the surfaces (a) without heating, (b) heating at 250 °C; (c) heating at 500 °C.

4.2. Bonding strength evaluation

After we clarified the surface conditions, we used these aluminum plates to fabricate aluminum/PA6 hybrids via injection insert molding. The bonding strength was measured. Fig. 5 shows the bonding strength results for the different surfaces. The bonding strength increased with the reduction of surficial adsorbed water. With the aluminum plates having the least surficial adsorbed water (heating at 500 °C), the bonding strength increased by approximately 50 %, indicating that the surficial adsorbed water is a critical factor for the bonding. In addition, we also compared the fracture energies for the aluminum/PA6 hybrids. The fracture energy was obtained by calculating the area under the displacement-force curve obtained during the tensile test. Fracture energy was used to compare with the adhesion energy calculated by MD. For the surfaces with the most, medium, the least water amount (without heating, heating at 250 °C, heating at 500 °C), the fracture energies were 54 ± 39 mJ, 78 ± 40 mJ, and 165 ± 61 mJ, respectively, for the 5 mm × 10 mm bonding area. The fracture energy change shows a similar trend as the bonding strength results. The sample having the least amount of surficial adsorbed water showed the highest fracture energy.

One debate regarding the bonding strength change may be that the heating may cause the structure change of the amorphous AlOOH, which contributed to the bonding strength increase. Here, the surfaces were observed with SEM and AFM, as shown in Fig. 6. SEM and AFM images show that the surface structures are almost the same before and after heating. It indicates that the heating did not result in the obvious structure change of the amorphous AlOOH on the aluminum surface. Also, the XPS results show that the chemical change of the amorphous AlOOH on surface is also minor. Such a minor change makes it difficult to explain the obvious increase in bonding strength. Therefore, we deduced that the bonding strength change results from the change of surficial adsorbed water, which is the most variable influencing factor among these aluminum plates. Some previous studies [9–12] also supported our deduction.

Since the existence of surficial adsorbed water on aluminum hinders its close contact with PA6 chains, it is assumed that the surface with less surficial adsorbed water is easier to let aluminum and PA6 contact closely to form hydrogen bonds or chemical bonds. Hydrogen bond/chemical bonds have more bonding energy compared with the Van der Waal force and the electrostatic force, which should be the reason for the increased bonding strength.

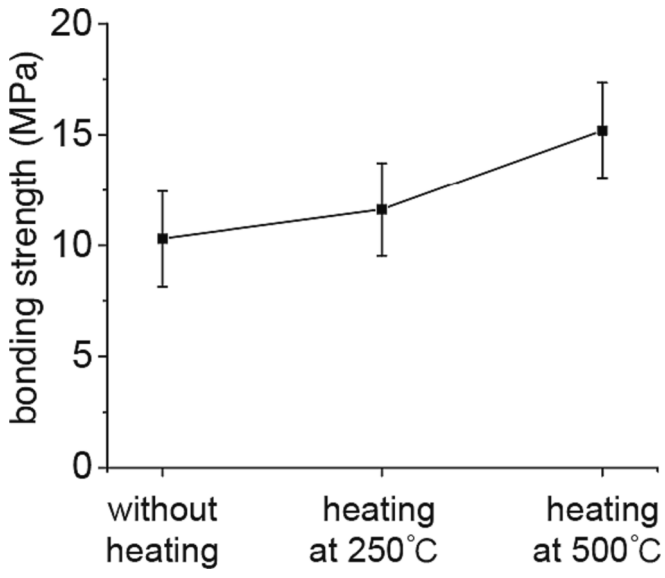

Fig. 5. Bonding strength of aluminum/PA6 hybrids with different surface water amounts.

To confirm the possible formation of the hydrogen bond/chemical bond, we observed the joining interface with AFM-IR. Before AFM-IR measurement, it is necessary to confirm which part of the aluminum/PA6 hybrid should be measured. As shown in Fig. 6, nanostructures formed on the aluminum surface. During the injection molding, PA6 infiltrates into these nanostructures, forming a bonding region where the amorphous AlOOH and PA6 are mixed. Fig. 7 (a) shows a cross-section image of the AFM results. It shows that the height of the nanostructures is approximately 100 nm. Fig. 7(b) shows a cross-section TEM image of the aluminum/PA6 hybrids. A 100 nm bonding region can be observed. Therefore, to measure the possible hydrogen bond/chemical bond, it is necessary to measure a position inside the 100 nm bonding region.

Here, AFM-IR was measured at various positions, as shown in the left panel of Fig. 8(a) and (b). The position at 25 nm, 50 nm, and 100 nm represents the bonding region where PA6 interacts with the amorphous AlOOH, which is the possible region to form hydrogen bond/chemical bond. The other position at 500 nm and 1000 nm represents the PA6 body. The measurement was performed within a wavenumber range of 2000 to 1000 cm^{-1}.

The right panels of Fig. 8(a) and (b) show the AFM-IR results for the joints made with the aluminum plates without heating and heating at 500 °C. The formation of the hydrogen bond/chemical bond was inspected by observing the change of –CONH functional group in PA6. In the spectrums in Fig. 8, peaks from C═O stretching at 1668 cm^{-1} and N–H bending at 1545 cm^{-1} were observed [25,26]. The hydrogen bond/chemical bond formation between –CONH and amorphous AlOOH should cause the increase/decrease or peak shift of these peaks.

As shown in Fig. 8(a), for the aluminum plate with a large amount of surficial adsorbed water (without heating), The changes from C═O stretching and N–H bending were not observed. Also, no new peak formation was observed. These results indicate that no hydrogen bond/chemical bond was formed between amorphous AlOOH and PA6. On the other hand, as shown in Fig. 8(b), for the aluminum plate with the least amount of surficial adsorbed water (heating at 500 °C), a new peak at 1630 cm^{-1} appeared at the right side of the C═O stretching peak. Also, the relative reduction of the C═O stretching at 1668 cm^{-1} was observed. The new peak at 1630 cm^{-1} can be assigned to the hydrogen-bonded C═O [25,26]. It indicates that hydrogen bonds formed between C═O in PA6 and amorphous AlOOH. In addition, the relative intensity between the hydrogen-bonded N–H bending and free N–H bending increased, indicating that hydrogen bond is also possible to form between N–H in PA6 and amorphous AlOOH. No new peak related to the possible chemical bond was found, indicating that the bonding strength increase should result from the hydrogen bond. These results confirmed the formation of hydrogen bonds between amorphous AlOOH and PA6, which well explained the increased bonding strength.

Theoretically, for the sample without heating, PA6 contacts with the water molecules on the surface. Forming hydrogen bonds between surficial water molecules and PA6 is possible. The other part of PA6 (the position at 1000 nm) cannot contact the water molecules on the surface. Therefore, the spectrum changes between the points at 25 nm and 100 nm should also be observed for the sample without heating. However, during the cross-section sample fabrication process, the whole interface is in contact with polishing water. The wet sample fabrication process may make the other PA6 part (the position at 1000 nm) absorb some water molecules, making the spectrum caused by the hydrogen bond between water molecules and PA6 undiscernible at different positions. Fortunately, the hydrogen bond between the AlOOH and PA6 is stronger than the hydrogen bond between water molecules and PA6 (can be verified by molecular dynamics simulations or first principal simulations). Therefore, even if the wet polishing process influences the detection of hydrogen bonds between water molecules and PA6, the hydrogen bond between AlOOH and PA6 is uninfluenced.

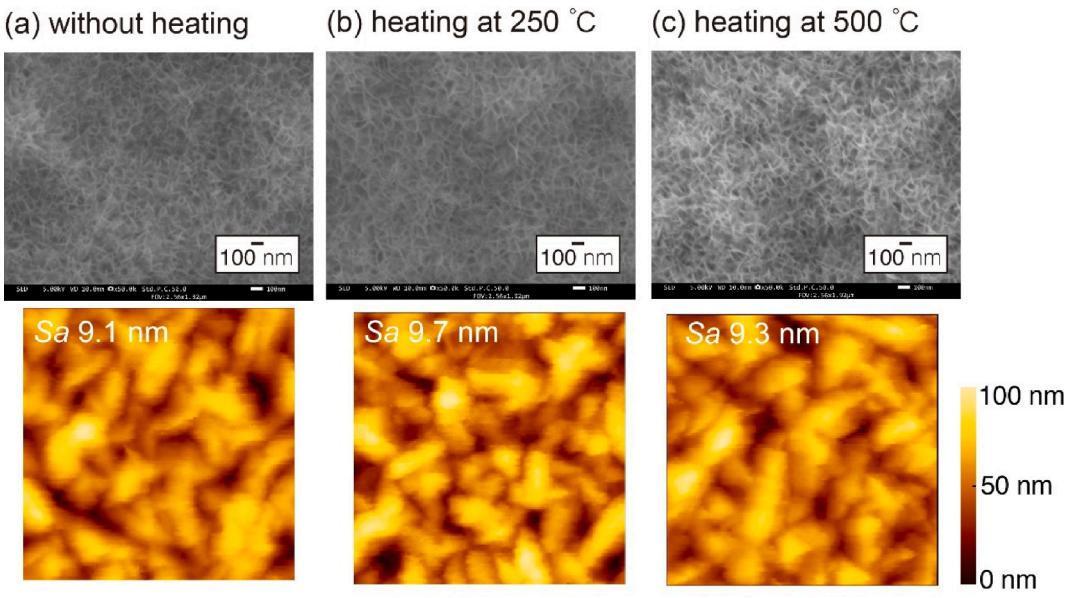

Fig. 6. SEM and AFM observation of the surfaces (a) without heating, (b) heated at 250 °C; (c) heated at 500 °C.

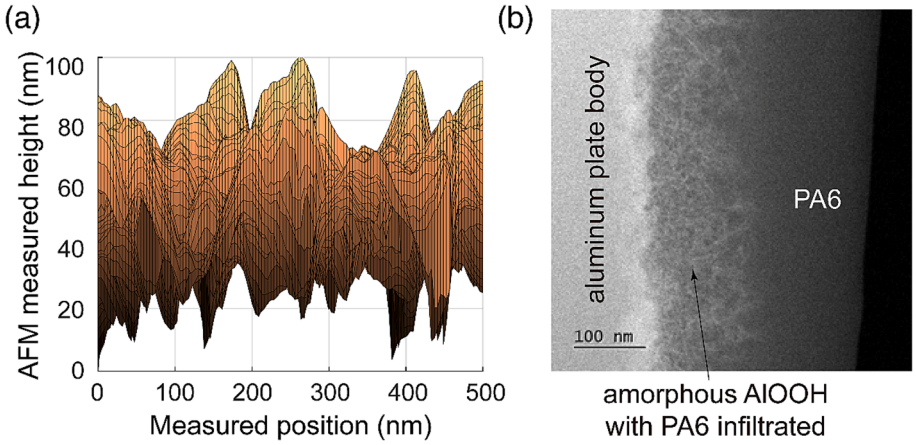

Fig. 7. (a) Side view of the AFM results for the nanostructures on aluminum; (b) TEM image of the cross-section of the aluminum/PA6 hybrid.

4.3. MD simulation

Fig. 9 shows the equilibrated results for the models with different amount of surficial adsorbed water indicated by the different numbers of water molecules. Blue circles were put around the water molecules to find them easier. For the results without water molecules, as shown in Fig. 9(a), close contact between amorphous AlOOH and PA6 was achieved. On the other hand, for the conditions with water molecules, as shown in Fig. 9(b-d), water molecules exist between amorphous AlOOH and PA6, blocking their close contact. However, it shows that water molecules can diffuse into PA6 to some extent. This kind of water molecule diffusion can reduce the water molecules between amorphous AlOOH and PA6, which provides space for PA6 to reach the amorphous AlOOH surface. In Fig. 9(b-d), the figures with water molecules hidden clearly show that with the increase of water molecules, the contact between amorphous AlOOH and PA6 reduced. Also, it shows that even if the water molecules exist, the contact between the amorphous AlOOH and PA6 cannot be blocked entirely. Such water molecules diffusion and contact formation may explain why the bonding of aluminum/PA6 can be achieved even if the water exists during the experiment.

Fig. 10(a) shows the water molecules distribution along the Z-axis after equilibration. Most of the water molecules reside on the amorphous AlOOH surface. Also, the water diffusion into PA6 is clearly observed. The water can be found approximately 2 nm away from the amorphous AlOOH surface, which is a distance much longer than its initial water model thickness (for the 600 water molecules conditions, its initial water model thickness is 0.9 nm). The contact between amorphous AlOOH and PA6 was also analyzed quantitatively. As shown in Fig. 10 (b), the number of close-contact atom pairs and hydrogen bonds reduced with the increase of water molecules, indicating the detrimental effect of surficial adsorbed water. Here, the close-contact atom pair is defined as donor-H/accepter pairs whose H-acceptor length is less than 0.35 nm but donor-H-acceptor bond angle is less than 150 degrees. For the close-contact atom pair, once its donor-H-acceptor bond angle is larger than 150 degrees, it was considered as a hydrogen bond. The results in Fig. 10 (b) indicate that the reason for the bonding strength increase should not result from the hydrogen bonding only. It shows that besides the formation of hydrogen bonds, the atom pair with closer contact is also achieved. The close contact increases the Van der Wall's force and the electrostatic force, which also contributes to the higher bonding strength.

The successful aluminum/PA6 hybrids should result from the bonding between the amorphous AlOOH and PA6. Here, we calculate the adhesion between amorphous AlOOH and PA6 to compare the

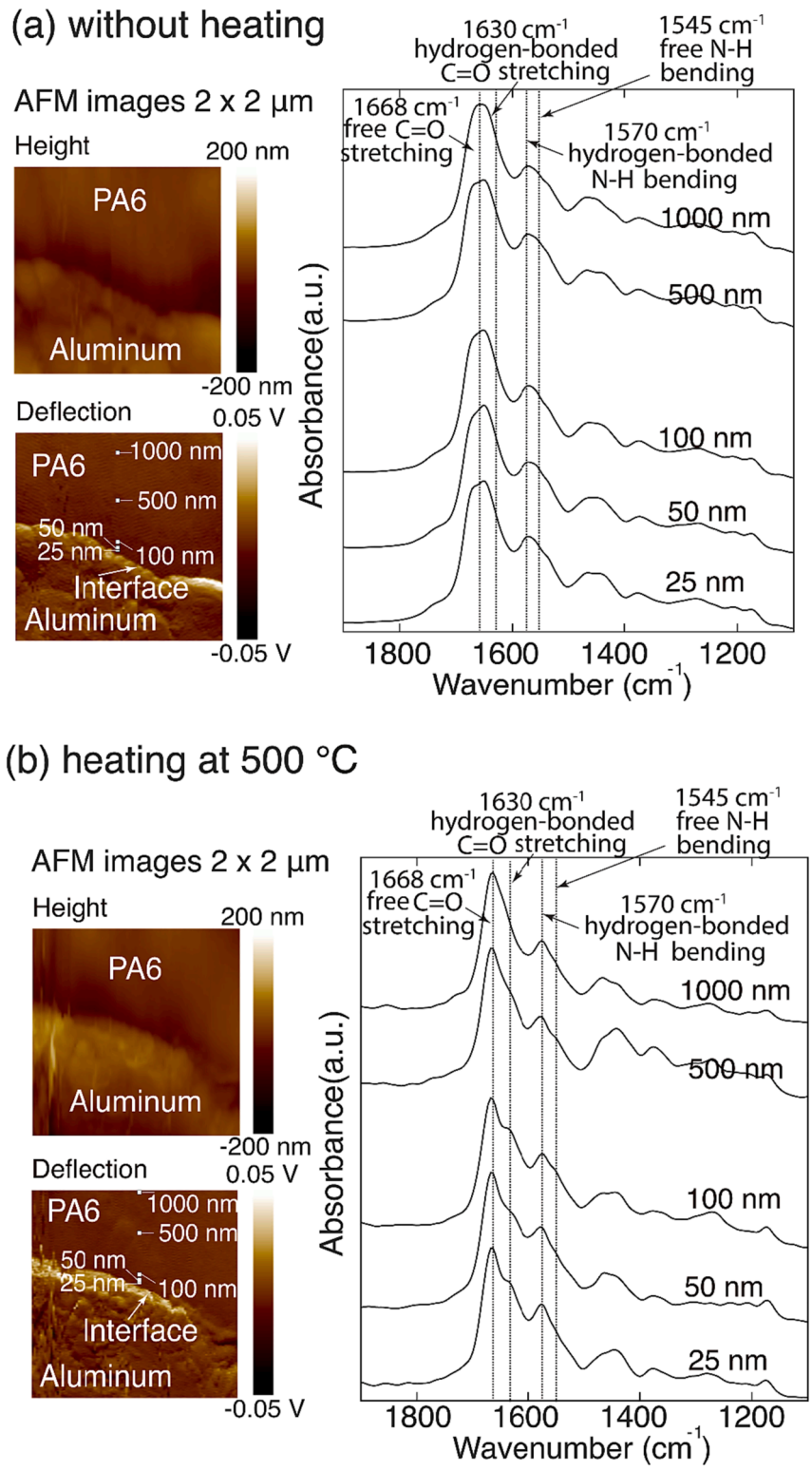

Fig. 8. Measurement positions and IR spectrums for AFM-IR results for surfaces (a) without heating and (b) heating at 500 °C.

simulation results with the experimental results. The results are shown in Fig. 11. It shows that the adhesion energy decreases with the increase amount of surficial adsorbed water (water molecule numbers), which shows a similar trend observed for the fracture energy during the experiments. Both experiment and simulation results indicate that reducing the surficial adsorbed water is beneficial for the bonding between aluminum and PA6.

4.4. Discussions

In this study, we revealed the importance of removing the surficial adsorbed water for the hybrid bonding with both experimental and simulation results. The existence of the surficial adsorbed water impedes the close contact between metal and plastic, reducing the adhesion energy. Our results show that the adhesion energy positively correlates with the reduction of surficial adsorbed water. Since the water

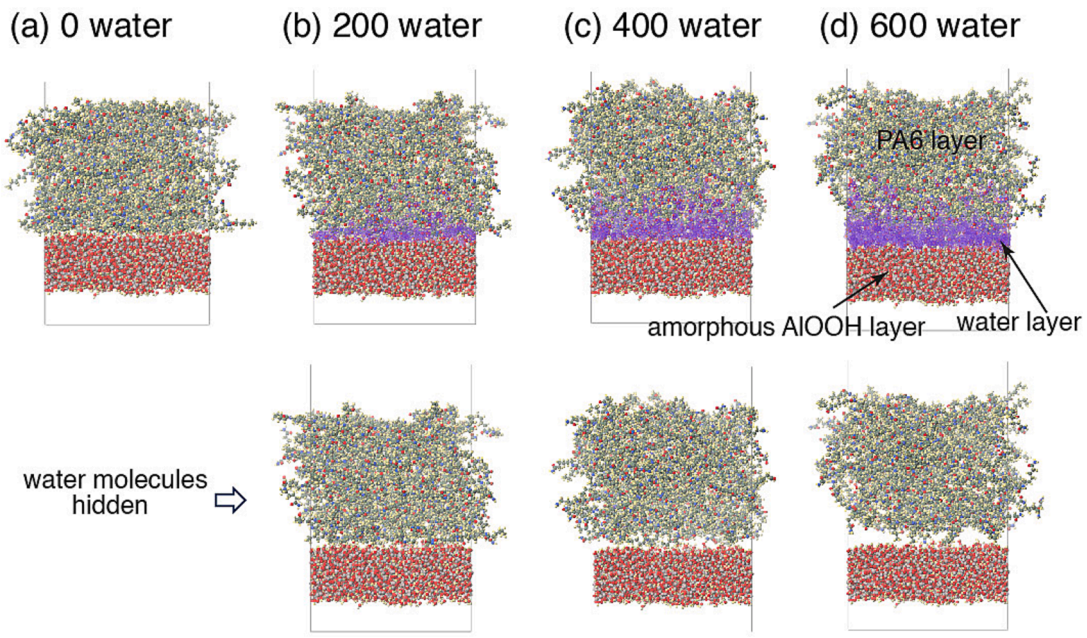

Fig. 9. The equilibrated results for the models with different numbers of water molecules; (a) without water; (b) with 200 water molecules; (c) with 400 water molecules; (d) with 600 water molecules.

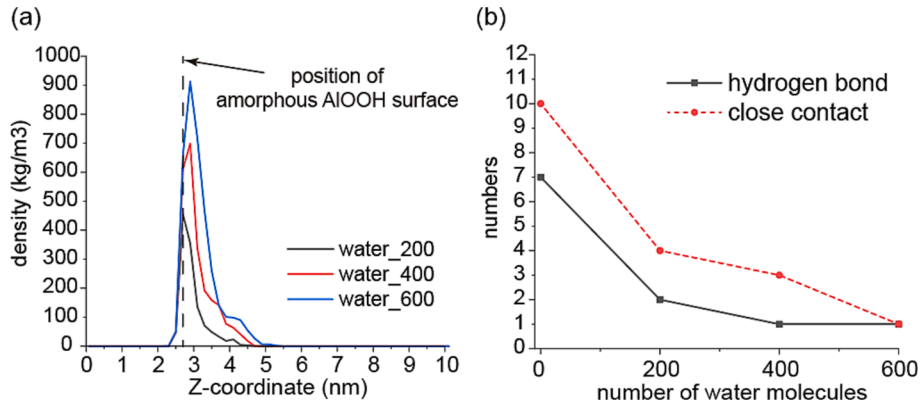

Fig. 10. (a) The water molecules distribution along Z-axis after equilibration; (b) The number of close-contact atom pairs and hydrogen bonds after equilibration for the models with different number of water molecules.

molecules do not fix in one position, they interact and partially diffuse into the plastic body, making it possible for plastic to contact metal closely even if some water molecules exist on the metal surface.

The reason for the bonding strength increase should result from more hydrogen bonds and more close-contact atom pairs. The simulation results found that the close contact atom pairs contribute to Van der Wall's force and the electrostatic force, but it is difficult to directly measure the close-contact atom pairs experimentally. Here, it suggests applying a combined experimental and simulation approach would be helpful to reveal the bonding mechanism for metal/plastic hybrids.

Only a limited number of previous studies discussed the influence of surficial adsorbed water on hybrid bonding. Most of these studies only did simulations. In our experiment, we used a high temperature to remove the surficial adsorbed water, aiming to produce surfaces with different water amounts. It does not mean that we suggest using such a high temperature of 500 °C for practical hybrid bonding. In practice, it should be effective to use a relatively low temperature, like 200 °C, because our results showed that as long as the surficial adsorbed water is reduced, the adhesion between metal and plastic should become better. Also, we found that the surficial adsorbed water was detected even after the heating at 500 °C. It is highly possible that the aluminum plate adsorbed surficial water again after heating. This phenomenon implies that it is also important to protect the metal from moisture before the hybrid bonding process.

5. Conclusions

This study clarified the influence of surficial adsorbed water on metal-plastic hybrids with a combined experimental and simulation approach. We achieved good agreement between experiment and simulation, finding that the surficial adsorbed water influences the metal-plastic hybrid bonding significantly. The conclusions are listed as follows:

- With the decrease in the amount of surficial adsorbed water, the bonding strength/fracture energy of the aluminum/PA6 hybrids increased.
- The reason for the higher bonding strength with less surficial adsorbed water is that more hydrogen bonds, stronger Van der Wall's force, and stronger electrostatic force were formed.

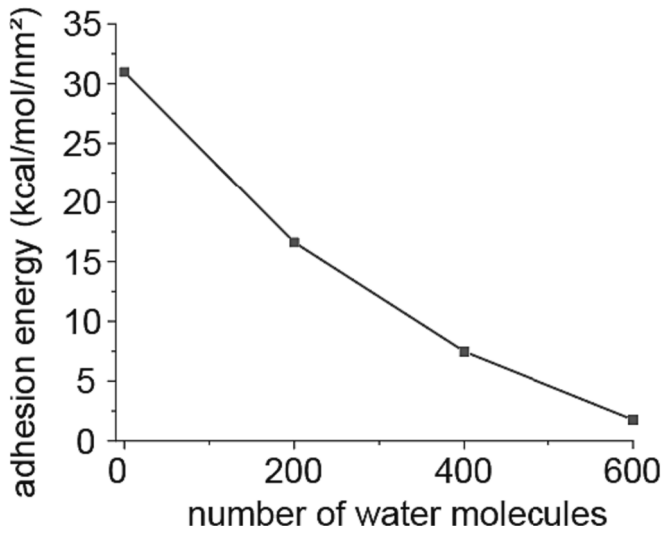

Fig. 11. The adhesion energy change for the models with different number of water molecules.

- The surficial water molecules on metal are movable, and they interact with and partially diffuse into PA6, making it possible for PA6 to contact metal closely even if some water molecules exist on the metal surface.
- The molecular dynamics simulation results show that the adhesion energy positively correlates with the reduction of surficial adsorbed water. It suggests that as long as the surficial adsorbed water is reduced, the adhesion between metal and plastic becomes better.

Our study focused on a very important but less-noticed surficial effect of the hybrid bonding. The results enriched the knowledge of metal-plastic hybrids, which would contribute significantly to hybrid bonding research and practical engineering.

CRediT authorship contribution statement

Shuaijie Zhao: Conceptualization, Data curation, Formal analysis, Funding acquisition, Investigation, Methodology, Validation, Visualization, Writing – original draft, Writing – review & editing. **Chuantong Chen:** Resources, Supervision, Writing – review & editing. **Hang Liang:** Resources, Writing – review & editing. **Shuohan Wang:** Data curation, Methodology. **Fuminobu Kimura:** Resources, Funding acquisition, Writing – review & editing. **Yusuke Kajihara:** Conceptualization, Project administration, Resources, Supervision, Writing – review & editing, Funding acquisition.

Declaration of competing interest

The authors declare that they have no known competing financial interests or personal relationships that could have appeared to influence the work reported in this paper.

Data availability

Data will be made available on request.

Acknowledgments

This work was supported Aluminum research grant program of Japan Aluminum Association. This work was also supported by JSPS KAKENHI (23K13559) and Foundation for the Promotion of Industrial Science, Japan. We thank the members of the Comprehensive Analysis Center, SANKEN, Osaka University for ToF-SIMS measurements. A part of This work was conducted at Advanced Characterization Nanotechnology Platform of the University of Tokyo, supported by "Nanotechnology Platform" of the Ministry of Education, Culture, Sports, Science and Technology (MEXT), Japan. The authors thank Prof. Hirahara and Prof. Sang at Iwate University for their help with AFM-IR.

References

[1] S. Zhao, F. Kimura, S. Kadoya, Y. Kajihara, Experimental analysis on mechanical interlocking of metal–polymer direct joining, Precis. Eng. 61 (2020), https://doi.org/10.1016/j.precisioneng.2019.10.009.
[2] S. Zhao, A. Takeuchi, F. Kimura, Y. Kajihara, Experimental investigation of the anchoring effect of aluminum/amorphous-plastics joints fabricated by injection molded direct joining, Precis. Eng. 77 (2022) 320–327.
[3] G. Bahlakeh, B. Ramezanzadeh, A detailed molecular dynamics simulation and experimental investigation on the interfacial bonding mechanism of an epoxy adhesive on carbon steel sheets decorated with a novel cerium–lanthanum nanofilm, ACS Appl. Mater. Interfaces 9 (2017) 17536–17551.
[4] D. Xin, Q. Han, Adhesion reliability of the epoxy-cu interface by molecular simulations, J. Adhes. 91 (2015) 409–418.
[5] S. Zhao, F. Kimura, S. Wang, Y. Kajihara, Chemical interaction at the interface of metal–plastic direct joints fabricated via injection molded direct joining, Appl. Surf. Sci. 540 (2021) 148339.
[6] X. Zou, K. Chen, H. Yao, C. Chen, X. Lu, P. Ding, M. Wang, X. Hua, A. Shan, Chemical reaction and bonding mechanism at the polymer-metal interface, ACS Appl. Mater. Interfaces. (2022) 27383–27396.
[7] P. Hirchenhahn, A. Al Sayyad, J. Bardon, A. Felten, P. Plapper, L. Houssiau, Highlighting chemical bonding between nylon-6.6 and the native oxide from an aluminum sheet assembled by laser welding, ACS Appl. Polym. Mater. 2 (2020) 2517–2527.
[8] S. Wang, F. Kimura, S. Zhao, E. Yamaguchi, Y. Ito, Y. Kajihara, Influence of fluidity improver on metal-polymer direct joining via injection molding, Precis, Eng 72 (2021) 620–626, https://doi.org/10.1016/J.PRECISIONENG.2021.07.001.
[9] H.A. Al-Abadleh, V.H. Grassian, FT-IR study of water adsorption on aluminum oxide surfaces, Langmuir. 19 (2003) 341–347.
[10] G. Rubasinghege, V.H. Grassian, Role (s) of adsorbed water in the surface chemistry of environmental interfaces, Chem. Commun. 49 (2013) 3071–3094.
[11] J. Van den Brand, S. Van Gils, P.C.J. Beentjes, H. Terryn, J.H.W. De Wit, Ageing of aluminium oxide surfaces and their subsequent reactivity towards bonding with organic functional groups, Appl. Surf. Sci. 235 (2004) 465–474.
[12] K. Yoshizawa, H. Murata, H. Tanaka, Density-functional tight-binding study on the effects of interfacial water in the adhesion force between epoxy resin and alumina surface, Langmuir. 34 (2018) 14428–14438.
[13] W. Cui, W. Huang, B. Hu, J. Xie, Z. Xiao, X. Cai, K. Wu, Investigation of the effects of adsorbed water on adhesion energy and nanostructure of asphalt and aggregate surfaces based on molecular dynamics simulation, Polymers (basel). 12 (2020) 2339.
[14] W. Sun, H. Wang, Moisture effect on nanostructure and adhesion energy of asphalt on aggregate surface: A molecular dynamics study, Appl. Surf. Sci. 510 (2020) 145435.
[15] V.A. Ranea, I. Carmichael, W.F. Schneider, DFT Investigation of Intermediate Steps in the Hydrolysis of $α$-Al2O3 (0001), J. Phys. Chem. C. 113 (2009) 2149–2158.
[16] S. Zhao, F. Kimura, E. Yamaguchi, N. Horie, Y. Kajihara, Manufacturing aluminum/polybutylene terephthalate direct joints by using hot water–treated aluminum via injection molding, Int. J. Adv. Manuf. Technol. (2020), https://doi.org/10.1007/s00170-020-05364-0.
[17] P. Godart, J. Fischman, K. Seto, D. Hart, Hydrogen production from aluminum-water reactions subject to varied pressures and temperatures, Int. J. Hydrogen Energy. 44 (2019) 11448–11458.
[18] T. Morimoto, M. Nagao, F. Tokuda, Desorbability of chemisorbed water on metal oxide surfaces. I. Desorption temperature of chemisorbed water on hematite, rutile and zinc oxide, Bull. Chem. Soc. Jpn. 41 (1968) 1533–1537.
[19] M. Egashira, M. Nakashima, S. Kawasumi, T. Selyama, Temperature programmed desorption study of water adsorbed on metal oxides. 2. Tin oxide surfaces, J. Phys. Chem. 85 (1981) 4125–4130.
[20] X. Krokidis, P. Raybaud, A.-E. Gobichon, B. Rebours, P. Euzen, H. Toulhoat, Theoretical study of the dehydration process of boehmite to $γ$-alumina, J. Phys. Chem. B. 105 (2001) 5121–5130.
[21] N. Senda, Development of molecular calculation support system "Winmostar", Idemitsu, Tech. Rep. 49 (2006) 106–111.
[22] A.P. Thompson, H.M. Aktulga, R. Berger, D.S. Bolintineanu, W.M. Brown, P. S. Crozier, P.J. in't Veld, A. Kohlmeyer, S.G. Moore, T.D. Nguyen, LAMMPS-a flexible simulation tool for particle-based materials modeling at the atomic, meso, and continuum scales, Comput. Phys. Commun. 271 (2022) 108171.
[23] S.P. Adiga, P. Zapol, L.A. Curtiss, Structure and morphology of hydroxylated amorphous alumina surfaces, J. Phys. Chem. C. 111 (2007) 7422–7429.
[24] E. McCafferty, J.P. Wightman, Determination of the concentration of surface hydroxyl groups on metal oxide films by a quantitative XPS method, Surf. Interface

Anal. Int. J. Devoted to Dev. Appl. Tech. Anal. Surfaces, Interfaces Thin Film. 26 (1998) 549–564.

[25] Y. Ma, T. Zhou, G. Su, Y. Li, A. Zhang, Understanding the crystallization behavior of polyamide 6/polyamide 66 alloys from the perspective of hydrogen bonds: projection moving-window 2D correlation FTIR spectroscopy and the enthalpy, RSC Adv. 6 (2016) 87405–87415.

[26] D. Surblys, T. Yamada, B. Thomsen, T. Kawakami, I. Shigemoto, J. Okabe, T. Ogawa, M. Kimura, Y. Sugita, K. Yagi, Amide A band is a fingerprint for water dynamics in reverse osmosis polyamide membranes, J. Memb. Sci. 596 (2020) 117705.